Ultrafast Optical Spectroscopy of Large-Momentum Excitons in GaAs

G. Göger,[1] M. Betz,[1] A. Leitenstorfer,[1] M. Bichler,[2] W. Wegscheider,[3] and G. Abstreiter[2]

[1]*Physik-Department E 11, Technische Universität München, D-85748 Garching, Germany*

[2]*Walter-Schottky-Institut, Technische Universität München, D-85748 Garching, Germany*

[3]*Institut für Angewandte und Experimentelle Physik, Universität Regensburg, D-93040 Regensburg, Germany*

(Received 22 February 2000)

Highly energetic excitons with wave vectors much larger than that of an absorbed photon are excited in thin GaAs films. We observe propagation beats between three polariton modes up to 300 meV above the absorption edge employing femtosecond transmission spectroscopy. The dispersion relations of the coherent excitations are measured. Ultrafast exciton damping via scattering with nonequilibrium carriers and with phonons is investigated. The dynamics is found to deviate strongly from the relaxation of free carriers. Theoretical simulations are in quantitative agreement with the data.

PACS numbers: 71.35.Cc, 71.36.+c, 72.15.Lh, 78.47.+p

It is usually assumed that first-order interband transitions in crystalline solids occur almost vertically in the band structure since the photon momentum is negligible compared to the reciprocal lattice vector. Especially, optical excitation and probing of free excitons in direct semiconductors is considered possible only near the center of the Brillouin zone. Absorption of photons with energies corresponding to the absorption continuum is believed to result exclusively in the creation of unbound electron-hole pairs with total momentum close to zero.

In this Letter, we demonstrate that these restrictions do not hold in general. Because of the symmetry break at any interface momentum conservation is not strictly valid. As a result, when electromagnetic radiation with frequency above the fundamental absorption edge is incident on a semiconductor, excitons with large wave vectors may be excited in addition to free electron-hole pairs. In time and energy resolved femtosecond transmission experiments we find spectral beats between a photonlike mode propagating with the velocity of light divided by the refractive index and weak coherent excitations having a phase velocity given by the excess energy and the effective mass of excitons.

Polariton phenomena arising from exciton-light coupling have drawn much theoretical attention [1–6] and have been investigated extensively in experiments [6–10] focusing on the frequency regime close to the fundamental resonance. For the first time, the high sensitivity of our novel femtosecond pump-probe technique allows a spectroscopic investigation of excitons with large momenta in the absorption continuum of semiconductors. We measure directly the ultrafast propagation times of coherent excitons through thin GaAs films, allowing a precise determination of exciton dispersions. The dynamics of light-hole (lh) and heavy-hole (hh) exciton damping resulting from scattering with photoinjected nonthermal carriers and longitudinal optical (LO) as well as acoustic phonons is studied.

We perform highly sensitive pump-probe experiments using a two-color femtosecond Ti:sapphire laser with two independently tunable synchronized pulse trains [11]. Our high purity samples were grown by molecular-beam epitaxy and consist of 500, 200, and 50 nm thick GaAs layers oriented along $\langle 100 \rangle$ followed by an $Al_{0.33}Ga_{0.67}As$ cladding layer. The films are antireflection coated on both sides, contacted to transparent sapphire substrates and kept at low lattice temperature T_L inside a cryostat. The role of an ultrashort optical pump pulse is to create free electron-hole pairs before or during the propagation of polaritons excited by a probe pulse. Via Coulomb scattering with the nonequilibrium carriers, the dephasing of the coherent excitations induced by the probe may be controlled in a well defined way. The time delayed 17 fs probe pulse is spectrally analyzed in a double monochromator after transmission through the sample (spectral resolution: 0.6 meV). Transmission changes due to the excitation pulse are detected in the energy range from the $1s$ exciton to excess energies of 300 meV above the band gap.

In Fig. 1(a) the pump induced transmission changes in the 500 nm specimen are shown versus probe photon energy, measured at a delay time of $t_D = 10$ ps after excitation of an electron-hole density of 3×10^{15} cm^{-3}. The 80 fs pump pulse is centered at a photon energy of 1.70 eV. The transmission changes around a probing energy of 1.509 eV are large and may be explained by the nonlinear-optical response of the fundamental exciton polariton resonance X [9]. At probe photon energies in the absorption continuum, i.e., above 1.513 eV, nonequidistant oscillations appear in the differential spectra. This phenomenon is explained as follows: When probe photons of energy $h\nu_{\mathrm{Probe}}$ (see inset of Fig. 2) are incident on the sample surface, the break of the translational symmetry of the crystal allows excitation of excitons with wave vectors much larger than that of the electromagnetic wave in vacuum. Via the electric dipole interaction, the excitonic polarization couples coherently to the light field resulting in new quasiparticles, called exciton polaritons. Near the fundamental resonance at an energy of 1.509 eV, the quasiparticles have both photonic and excitonic character. For excess energies of a few meV, the photonlike polariton

 0031-9007/00/84(25)/5812(4)$15.00

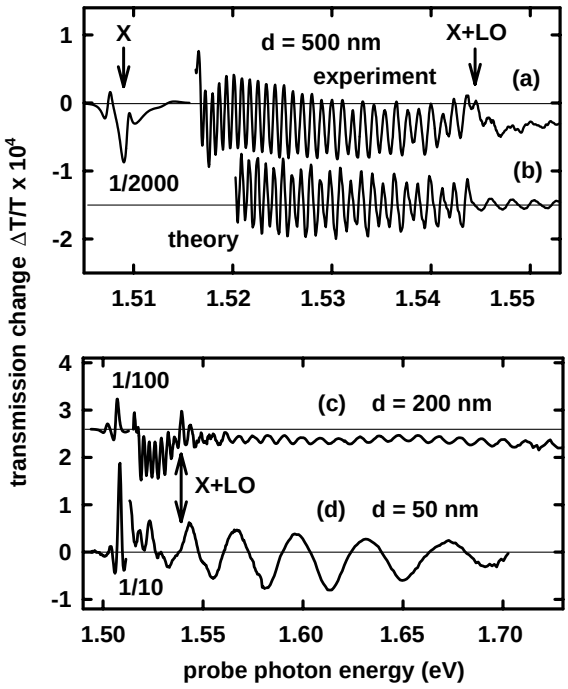

FIG. 1. Spectrally resolved transmission changes measured 10 ps after hot carrier injection in GaAs films of different thicknesses d at $T_L = 20$ K [(a), (c), and (d)]. Free carrier densities are $N_{\text{pump}} = 3 \times 10^{15}$ cm^{-3} (a), 5×10^{15} cm^{-3} (c), and 3×10^{16} cm^{-3} (d), respectively. (b) Transmission changes as calculated theoretically for the $d = 500$ nm specimen.

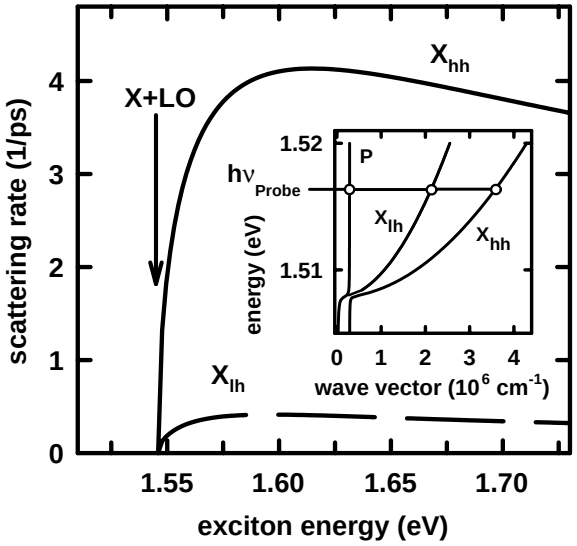

FIG. 2. Calculated LO phonon emission rates of 1s hh (X_{hh}, full line) and lh (X_{lh}, dashed line) excitons in GaAs at $T_L = 0$ K, assuming parabolic bands. Inset: Exciton polariton dispersion consisting of one photonlike branch (P) and two excitonlike branches (X_{lh}, X_{hh}).

branch P approaches a steep dispersion relation with slope proportional to the inverse index of refraction. Simultaneously the hh and lh excitonlike polaritons (X_{hh} and X_{lh} in the inset of Fig. 2) recover their parabolic exciton center-of-mass dispersion. Frequency components of the incident pulse corresponding to an energy far above the fundamental exciton are converted predominantly into photonlike polaritons. Only a small fraction propagates on the excitonlike branches. Disregarding scattering of the polaritons inside the medium, the three components travel unattenuated to the other sample surface and are reconverted into photons. Interference of the electric field amplitudes results in weak fringes superimposed on the spectrum of the transmitted probe pulse. The spectral beats reflect the different phase velocities of the polaritons which are proportional to the inverse wave vectors at the intersection points of the photon energy with the three branches (see inset of Fig. 2). The efficient damping of excitonlike polarizations via the scattering with free carriers injected by the pump pulse modifies the fringe contrast in the probe beam. Therefore, the nonlinear optical experiments are very sensitive to polariton effects: Our photomodulation technique measures the difference between the transmitted probe spectra with and without excitation and avoids the background problems which would be faced in linear transmission. In this way, both stationary aspects like exciton dispersions as well as dynamical properties such as exciton-carrier scattering rates become accessible.

Two distinct components are identified in Fig. 1: One fast beating mode corresponding to the 1s hh exciton polariton, whose amplitude and period exhibit a sharp discontinuity at a probe photon energy of the fundamental 1s exciton plus one LO phonon (X + LO, $\hbar\omega_{\text{LO}} = 36$ meV in GaAs). Slower oscillations without steplike behavior at X + LO are superimposed originating from the lh exciton polariton. Apparently, a significant difference exists concerning the interaction of lh and hh excitons with LO phonons. lh excitons conserve their polarization over large distances high above the LO threshold energy [see Figs. 1(c) and 1(d)], while the coherence of hh excitons is destroyed rapidly.

In order to analyze our experimental findings, we have performed extensive numerical simulations. Our model is based on the Pekar-Hopfield additional boundary conditions demanding the vanishing of both hh and lh excitonic polarization at the surfaces of the sample [3,8]. Only 1s hh and lh excitons are included and the damping of the photonlike branch by the injected carriers is neglected [12]. We estimate a pump induced exciton-carrier scattering rate of 1 ps^{-1} for the excitonlike branches [13]. Polar-optical scattering of excitons with LO phonons is described by the following matrix element [14]:

$$|\langle 1s,\vec{K}|H_{X,\text{LO}}|1s,\vec{K}-\vec{q}\rangle|^2 = \frac{\hbar\omega_{\text{LO}}e^2}{2Vq^2}\left(\frac{1}{\epsilon_\infty}-\frac{1}{\epsilon_0}\right)\times\left\{\left[1+\left(\frac{qa_Bm_h}{2(m_e+m_h)}\right)^2\right]^{-2}-\left[1+\left(\frac{qa_Bm_e}{2(m_e+m_h)}\right)^2\right]^{-2}\right\}^2. \quad (1)$$

In contrast to the polaron coupling of free carriers, a form factor appears containing the mass ratio of electrons and holes [curly bracket in the right-hand side of Eq. (1)]. The spontaneous LO emission rate calculated for GaAs is shown in Fig. 2: *hh* excitons couple strongly to an LO polarization field and scatter with a rate of approximately 4 ps^{-1} above the threshold energy for LO emission. On the other hand, *lh* excitons with their similar electron and hole masses behave almost like neutral particles. Therefore, we obtain an LO phonon emission rate below 0.3 ps^{-1}. In case of identical masses of electron and hole the polar-optical Fröhlich interaction between 1*s* states vanishes exactly. The result of a simulation based on this model is shown in Fig. 1(*b*): In good agreement with the experimental data in Fig. 1(*a*), both *hh* and *lh* excitons contribute to the spectral beats below an energy of $X + \mathrm{LO}$. Above threshold, the *hh* component is strongly reduced and the *lh* beats remain. The beating frequency depends very sensitively on the dispersion relation: From the data in Figs. 1(*a*) and 1(*c*), we determine a *hh* exciton effective mass of $0.52m_0$ in the $\langle 100 \rangle$ direction. For the *lh* exciton mass a value of $0.19m_0$ is found, also reproducing the *hh*-*lh* beating structure near $X + \mathrm{LO}$ [see Fig. 1(*b*)]. In the 200 nm sample [Fig. 1(*c*)], the *lh* polariton beating is observable for probe photon energies up to 1.8 eV and the high energy region of the dispersion may be examined. It turns out that for excess energies larger than 200 meV the oscillation periods increase significantly slower than expected for a constant effective *lh* exciton mass. This effect is ascribed to the nonparabolicity of the conduction and *lh* bands.

A polariton interference spectrum of the 50 nm GaAs layer is presented in Fig. 1*(d)*. As in the thicker samples, we find a discontinuity at a probe photon energy of $X + \mathrm{LO}$, separating a low energy region containing two beating components from the high energy regime with only the *lh* interference structure. Though the transit time through the sample has decreased by a factor of 10 compared to the 500 nm specimen, LO phonon emission still leads to an effective damping of the *hh* polariton wave packet. Since the propagation length in the 50 nm specimen approaches the excitonic Bohr radius, period and amplitude of the oscillations depend crucially on the microscopic properties of the excitonic polarizability near the semiconductor interfaces. A quantitative simulation of these data would have to take into account an exciton-free surface layer and a quantized center-of-mass motion [1,6,15].

Another indication for the splitting of an ultrashort probe pulse into three components propagating according to different dispersion relations is obtained by examining the wave packet dynamics at various negative delay times t_D, when the arrival of the probe pulse at the sample surface precedes that of the pump pulse. In Fig. 3 the pump induced transmission changes in the 500 nm sample are plotted versus probe photon energy. At time delays of $t_D = 1$ ps and $t_D = 0$ ps, both *hh* and *lh* probe polaritons suffer efficient damping. Since they propagate at a lower group velocity than the photonlike component of the pump pulse, the excitonlike wave packets scatter with pump generated free electrons and holes along the entire crystal thickness. If the probe pulse enters the sample at $t_D = -2$ ps, i.e., before the injection of scattering partners, the spectrum contains exclusively one component (*hh* excitons), ending at a photon energy of $X + \mathrm{LO}$. The other mode (*lh* excitons) with group velocity larger than 500 nm/2 ps escapes the sample before carrier excitation by the pump. For a delay time of $t_D = -3.5$ ps, the *hh* excitons are damped only towards the end of their propagation through the film and the differential beat amplitude is strongly reduced.

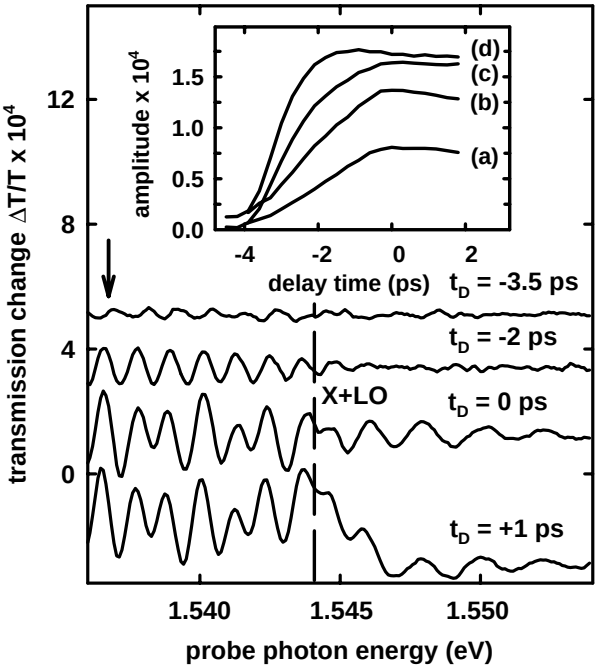

FIG. 3. Differential transmission spectra of the 500 nm GaAs layer near probe photon energies of $X + \mathrm{LO}$ for different delay times t_D. Pump and probe intensities are chosen as in Fig. 1(*a*). Inset: Amplitude of the spectral oscillation versus delay time extracted at a probe photon energy of 1.533 eV (vertical arrow) and at different free carrier excitation densities N_{pump} of 6×10^{14} cm^{-3} (*a*), 2×10^{15} cm^{-3} (*b*), 4×10^{15} cm^{-3} (*c*), and 1×10^{16} cm^{-3} (*d*).

The delay dependent oscillation amplitude reflects the damping dynamics of the excitonlike polaritons: The temporal evolution of the oscillation amplitude of the *hh* component is shown in the inset of Fig. 3, measured for different excitation densities at a probe photon energy of 1.533 eV (marked by a vertical arrow). The identical onset of the spectral oscillations corresponds to a transit time of 3.8 ps, confirming the effective *hh* exciton mass of $0.52m_0$. The dynamics of the time resolved oscillation amplitude depends strongly on carrier density: At low densities of 6×10^{14} and 2×10^{15} cm^{-3} [transients (*a*) and (*b*) in the inset of Fig. 3], the pump inferred dephasing causes an almost linear decrease of the coherent *hh* exciton

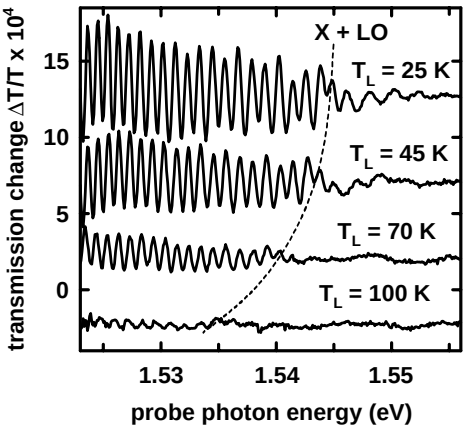

FIG. 4. Spectrally resolved transmission changes for the 500 nm thick GaAs sample, measured at $t_D = +10$ ps for various lattice temperatures T_L. Pump and probe injected densities are $N_{\text{pump}} = 5 \times 10^{15}$ cm^{-3} and $N_{\text{probe}} = 1 \times 10^{14}$ cm^{-3}, respectively.

polarization with increasing delay time. The integral damping reaches its maximum value at zero delay. Raising the pump density up to 1×10^{16} cm^{-3} [transients (*c*) and (*d*) in Fig. 3], the sample thickness starts to exceed the mean-free path for exciton-carrier scattering. Even for small interaction lengths, or equivalently for early delay times, the excitonlike polariton is substantially weakened. From the initial slope at $t_D = -3.8$ ps, the time constant for exciton dephasing via collisions with free carriers may be deduced, assuming an exponential polarization decay: As an example, we measure a damping time of 1.5 ps for an electron-hole density of 1×10^{16} cm^{-3}. The oscillation amplitude saturates at carrier densities above 1×10^{16} cm^{-3} and the *hh* exciton polariton is completely damped out [Figs. 3(*c*) and 3(*d*)]. From the saturation value of the fringe contrast we conclude that the splitting ratio for the polarization amplitudes of the *hh* excitonlike branch and the photonlike branch is 2×10^{-4} at an excess energy of 25 meV.

Differential transmission spectra have also been studied as a function of temperature; see Fig. 4: The results obtained with the 500 nm sample at a delay time of $t_D = 10$ ps show an increasing redshift of the $X + \text{LO}$ threshold with temperature due to band gap renormalization (see dashed line as a guide for the eye). Simultaneously, the oscillation amplitude decreases. At temperatures above 100 K the propagation beats vanish due to the efficient exciton dephasing via acoustic phonon scattering. From an analysis of the oscillation amplitude, we extract an estimate for the linear coefficient σ of the increase of the homogeneous exciton linewidth with temperature. We deduce $\sigma = 20$ μeV/K, in surprising agreement with the value of $\sigma = 17$ μeV/K found for the $1s$ exciton with negligible center-of-mass motion [16].

In conclusion, we have found a spectroscopic handle to study the dynamics of excitons with large kinetic energy in direct-gap semiconductors. A wealth of new information is obtained on these fundamental electronic excitations which have up till now not been accessible experimentally. Polariton interferences in GaAs films, monitored by ultrasensitive differential transmission spectroscopy, enable us to derive the dispersion relation of *hh* and *lh* excitons. Turning our attention to the dephasing of the excitonic polarization, we find that scattering with acoustic phonons does not depend significantly on the excess energy and is of comparable strength for *lh* and *hh* excitons. In contrast, the relaxation of *lh* excitons via LO phonon emission is significantly slower as compared to *hh* excitons. This striking difference is explained by the reduced polaron coupling for excitons with similar electron and hole masses. For film thicknesses much larger than the excitonic Bohr radius, Pekar's additional boundary conditions account quantitatively for the observed oscillations. Significant deviations occur in very thin samples: In future studies, a comparison of the experimental data with more elaborate microscopic model calculations should allow a refined insight into the electrodynamics of solid state interfaces.

We thank W. Kaiser, L. V. Keldysh, A. Laubereau, E. Muljarov, and R. Zimmermann for valuable discussions. This work has been supported by the DFG via the Schwerpunktprogramm "Quantenkohärenz in Halbleitern."

[1] For an overview see *Excitons in Confined Systems*, Proceedings of the International Meeting, Rome, 1987, edited by R. Del Sole, A. D'Andrea, and A. Lapiccirella (Springer, Berlin, 1988); M. Ueta, H. Kanzaki, K. Kobayashi, Y. Toyozawa, and E. Hanamura, *Excitonic Processes in Semiconductors* (Springer, Berlin, 1986).
[2] J. J. Hopfield, Phys. Rev. **112**, 1555 (1958).
[3] S. I. Pekar, Sov. Phys. JETP **34**, 1176 (1958).
[4] K. Henneberger, Phys. Rev. Lett. **80**, 2889 (1998).
[5] A. Stahl, Phys. Status Solidi (b) **106**, 575 (1981).
[6] J. Tignon *et al.*, Phys. Rev. Lett. **84**, 3382 (2000).
[7] V. A. Kiselev, B. S. Razbirin, and I. N. Uraltsev, Phys. Status Solidi (b) **72**, 161 (1975).
[8] A. Tredicucci *et al.*, Phys. Rev. B **47**, 10 348 (1993).
[9] A. C. Schäefer and D. G. Steel, Phys. Rev. Lett. **79**, 4870 (1997).
[10] S. Nüsse *et al.*, Phys. Rev. B **55**, 4620 (1997).
[11] C. Fürst, A. Leitenstorfer, and A. Laubereau, IEEE J. Sel. Top. Quantum Electron. **2**, 473 (1996).
[12] A rigorous theoretical treatment including higher exciton states and the Sommerfeld-enhanced continuum will be presented in a forthcoming paper by E. Muljarov and R. Zimmermann.
[13] C. Erginsoy, Phys. Rev. **79**, 1013 (1950).
[14] Y. Toyozawa, Prog. Theor. Phys. **12**, 111 (1959).
[15] A. D'Andrea and R. Del Sole, Phys. Rev. B **41**, 1413 (1990).
[16] L. Schultheis *et al.*, Phys. Rev. B **34**, 9027 (1986).